RESEARCH ARTICLE



Check for updates

Elucidation of the relationship between solid-state photoluminescence and crystal structures in 2,6-substituted naphthalene derivatives

Minoru Yamaji¹ | Isao Yoshikawa² | Toshiki Mutai³ | Hirohiko Houjou^{2,4} Kenta Goto⁵ | Fumito Tani⁵ | Kengo Suzuki⁶ | Hideki Okamoto⁷

Correspondence

Minoru Yamaii, Division of Materials and Environment, Department of Applied Chemistry, Graduate School of Science and Engineering, Gunma University, Ota, Gunma 373-0057, Japan.

Email: yamaji@gunma-u.ac.jp

Funding information

Cooperative Research Program of the Network Joint Research Center for Materials and Devices; Japan Society for the Promotion of Science, Grant/Award Numbers: JP18H02043, JP20K05648, JP23K04877; General Incorporated Foundation Monodzukuri Research Organization (MRO), established by Ota Chamber of Commerce & Industry, Gunma University and Ota City in Gunma, Japan; Association for the Advancement of Science & Technology, Gunma University

Abstract

Polycyclic aromatic hydrocarbons (PAHs) are known to exhibit fluorescence in solution, but generally do not emit in the solid state, with the notable exception of anthracene. We previously reported that PAHs containing multiple chromophores show solid-state emission, and we have investigated the relationship between their crystal structures and photoluminescence properties. In particular, PAHs with herringbone-type crystal packing, such as 2,6-diphenylnaphthalene (DPhNp), which has a slender and elongated molecular structure, exhibits redshifted solid-state fluorescence spectra relative to their solution-phase counterparts. In this study, we synthesized 2,6-naphthalene derivatives bearing phenyl and/or pyridyl substituents (PhPyNp and DPyNp) and observed distinct, redshifted emission in the solid state compared with that in solution. Crystallographic analysis revealed that both PhPyNp and DPyNp adopt herringbone packing motifs. These findings support our hypothesis that the spectral characteristics of PAH emission are closely linked to crystal packing arrangements, providing a useful strategy for screening PAH candidates for applications in organic semiconducting materials.

KEYWORDS

herringbone, polycyclic aromatic hydrocarbon, solid-state emission

This is an open access article under the terms of the Creative Commons Attribution License, which permits use, distribution and reproduction in any medium, provided the original work is properly cited.

J Chin Chem Soc. 2025;1-8. http://www.jccs.wiley-vch.de

¹Department of Applied Chemistry, Division of Materials and Environment, Graduate School of Science and Engineering, Gunma University, Ota, Gunma, Japan

²Department of Materials and Environmental Science, Institute of Industrial Science, The University of Tokyo, Meguro, Tokyo, Japan

³Technology Transfer Service Corporation, Minato, Tokyo, Japan

⁴Environmental Science Center, The University of Tokyo, Bunkyo, Tokyo, Japan

⁵Institute for Materials Chemistry and Engineering, Kyushu University, Fukuoka, Japan

⁶Hamamatsu Photonics K.K, Joko-cho, Hamamatsu, Shizuoka, Japan

⁷Department of Chemistry, Faculty of Environment, Life, Natural Sciences and Technology, Okayama University, Okayama, Japan

^{© 2025} The Author(s). Journal of the Chinese Chemical Society published by The Chemical Society Located in Taipei and Wiley-VCH GmbH.

1 | INTRODUCTION

Photoluminescence from aromatic molecules is among the most captivating phenomena that have attracted extensive investigation by organic chemists. Photophysical studies of polycyclic aromatic hydrocarbons (PAHs), which are composed of fused benzene rings, have traditionally been conducted in solution through measurements of their spectra, fluorescence quantum yields (Φ_f), and lifetime (τ_f) of prompt emission [1–3]. In contrast, solid-state emission from most typical PAHs such as naphthalene, phenanthrene, and pyrene, is generally negligible, with the notable exception of anthracene [4]. Recent advances in spectrometric techniques have significantly facilitated the accurate determination of Φ_f and τ_f values for emissive compounds not only in solution but also in the solid state [5]. In our previous study, we reported that biaryls consisting of naphthalene, phenanthrene, and pyrene chromophores exhibited emission in the solid state with higher Φ_f values compared with those in solution [6]. We observed that these biaryl compounds adopted herringbone packing motifs in the solid state, which was accompanied by red-shifted emission spectra relative to those observed in solution. This prompted us to investigate the relationship between crystal packing motifs and photophysical properties. Further evidence was provided by solid-state fluorescence observed in diphenylnaphthalene derivatives, naphthalene cores bearing multiple chromophores whose crystal structures could be broadly classified into two types: herringbone and stacked columnar arrangements [7]. For instance, 2,6-diphenylnaphthalene, which crystallized in a herringbone motif, exhibited a noticeable red shift in the solidstate emission, whereas other diphenylnaphthalenes with stacked columnar structures showed minimal spectral shift between solution and solid states. These findings led us to hypothesize a correlation: if a compound bearing multiple aromatic chromophores exhibits a significant red shift in solid-state emission compared with its solution-state counterpart, the crystal structure is likely to feature a herringbone motif. To examine the validity of this hypothesis, we turned to literature examples involvanthracene derivatives. 2,6-diphenylanthracene, a well-known organic semiconductor [8-13], exhibits red-shifted solid-state emission and crystallizes in a herringbone structure. This compound shares a slender and rod-like molecular shape with 2,6-diphenylnaphthalene. Similar characteristics, including semiconductive behavior and herringbone packing, are also investigated in 2,6-dipyridylanthracene, which possesses a comparable rod-like molecular geometry [14-17] although the solid-state emission is not reported to our best knowledge. One of the current trends

in organic materials research involves the development of multifunctional organic compounds capable of optical emission, charge transport, and electronic performance, particularly for use in organic field-effect transistors (OFETs) [18]. If our proposed structure-property relationship holds, it could serve as a useful screening criterion on designing organic semiconducting materials. Solid-state photoluminescence spectral shifts could serve as an indicator of favorable crystal packing, such as herringbone motifs, which are often associated with efficient charge transport properties [19–21].

In this context, we are engaged in elucidating the relationship between solid-state photophysical behavior and crystal structures of emissive organic molecules [22–24]. To date, relatively few PAHs are known to exhibit efficient solid-state photoluminescence. In the present study, we prepared two naphthalene-based compounds, 2-phenyl-6 pyridylnaphthalene (PhPyNp) and 2,6-dipyridylnaphthalene (DPyNp) along with 2,6-diphenylnaphthalene (DPhNp) (see Scheme 1 for the chemical structures), and investigated the solid-state photoluminescence. We determined the Φ_f and τ_f values in solution and the solid state, analyzed their crystal structures, and discussed the correlations between their photophysical properties and packing motifs.

2 | EXPERIMENTAL

The studied DArNps were prepared according to the procedures described in Data S1. Chloroform, acetonitrile, and ethanol (spectroscopic grade from Wako) were used as solvents for the spectral measurements without further purification. The NMR spectra for the DArNps recorded on a JEOL JNM-ECZ600R (600 MHz) spectrometer are deposited as Figures S2-S5. High-resolution fast atom bombardment mass spectra (HR-FAB-MS) were obtained using 3-nitrobenzyl alcohol as a matrix, and recorded on a double-focusing magnetic sector mass spectrometer (JEOL JMS-700). The absorption spectra in solution were recorded using a JASCO V-730 spectrophotometer. Fluorescence quantum yields (Φ_f) and fluorescence spectra in solution and in the solid state were obtained using an absolute photoluminescence quantum yield measurement system (Quantaurus-QY Plus, C13534-01) from HAMA-MATSU PHOTONICS K.K., whereas fluorescence lifetimes (τ_f) in solution and the solid state were determined using a time-correlated single-photon counting fluorimeter system (C16361-01) from HAMAMATSU PHOTONICS K.K. Samples in a quartz cuvette with a 1 cm optical path length were subjected to measurements for Φ_f and τ_f in aerated solution. The concentration of the solution for absorption measurement was adjusted by the maximum absorbance being less than 1.0, whereas that for emission

2192649, 0, Downloaded from https://onlinelibrary.wilej.com/doi/10.1002/jccs.70063 by Okayama University, Wiley Online Library on [2608/2025]. See the Terms and Conditions (https://onlinelibrary.wiley.com/terms-and-conditions) on Wiley Online Library for rules of use; OA articles are governed by the applicable Creative Commons Licensea

SCHEME 1 Molecular structures and abbreviations of diarylnaphthalenes (DArNps) studied in this work.

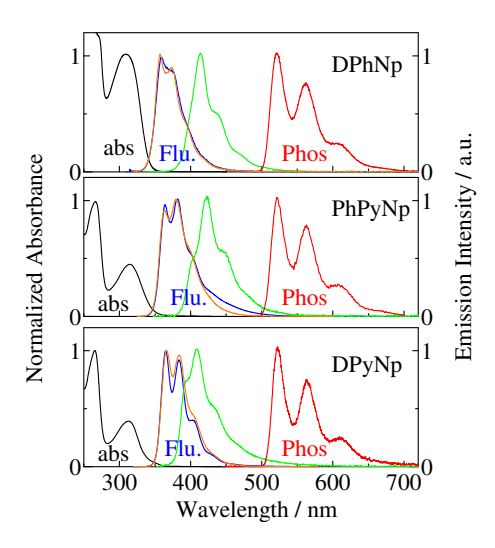


FIGURE 1 Absorption (black) and fluorescence spectra in chloroform (blue) at 295 K, fluorescence spectra in acetonitrile (orange), and the solid state (green) at 295 K and phosphorescence spectra (red) in ethanol at 77 K for DArNps. The emission spectra are not corrected.

measurements was adjusted by the absorbance at the excitation wavelength being close to 0.1. Single-crystal X-ray diffraction data were collected on a Rigaku XtaLAB P200, λ (Cu-K α) = 1.54184 Å. The structure was solved by direct method (SHELXS-2013 [25]) and refined on F^2 by fullmatrix least-squares techniques (SHELXL-2018 [26]), controlled by the Yadokari-XG software package [27]. The theoretical calculations for the studied DPNs were carried out at the DFT level, using the Gaussian 09 software package [28]. The geometries of the studied compounds were fully optimized using the 6-31G(d,p) basis set at the B3LYP method on the self-consistent reaction field (SCRF) theory using a conductor-like polarizable continuum model (CPCM) considering the dielectric constant of chloroform. The atom coordinates for the optimized geometries were deposited in SI. Time-dependence DFT (TD-DFT) calculations were performed at TD-B3LYP/6-31 + G(d,p) level using the optimized geometries.

3 RESULTS AND DISCUSSION

Spectroscopic features 3.1

Figure 1 shows the absorption and emission spectra of the DArNps studied in this work. The UV absorption spectra

of PhPyNp and DPyNp, each displaying two distinct absorption bands, closely resemble that of DPhNp. These observations suggest that the electronic structures of the studied DArNps are largely similar, regardless of the nature of the substituted π -electron systems. However, substitution with pyridyl group(s) induces a red shift in the absorption spectra compared with DPhNp. In solution, the studied DArNps exhibited fluorescence in the deepblue region (340-440 nm), while in the solid state, the emission spectra are red-shifted relative to those in solution. Both solution- and solid-state fluorescence spectra show vibrational structures, and the spectral profiles are generally consistent across the series of compounds. These findings indicate that the observed emission originates from a local excited state within the DArNp chromophore, rather than from excimer formation or intermolecular $\pi - \pi^*$ interactions between the neighboring substituted p-systems and the naphthyl core. Furthermore, the similarity of fluorescence spectra in acetonitrile and chloroform suggests that the emissive states possess minimal charge-transfer character. The observation of phosphorescence supports the occurrence of intersystem crossing from the lowest excited singlet state (S₁) to the triplet in the studied compounds. The characteristic 0-0 transition wavelengths (λ_f^{0-0}) of fluorescence for the DArNps, along with their corresponding fluorescence quantum yields (Φ_f) and lifetimes (τ_f), are summarized in Table 1.

The rates of the fluorescence (k_f) and nonradiative $(k_{\rm nr})$ processes were determined using Equations (1) and (2), respectively, as summarized in Table 1.

$$k_{\rm f} = \Phi_{\rm f} \tau_{\rm f}^{-1} \tag{1}$$

$$k_{\rm nr} = (1 - \Phi_{\rm f}) \tau_{\rm f}^{-1}$$
 (2)

The rates, k_f and k_{nr} determined in solution and in the solid state provide essential insight into the photophysical properties of the studied DArNps. Notably, the k_f values for PhPyNp and DPyNp were higher than that of DPhNp, suggesting that the replacement of the phenyl ring with pyridyl rings enhances radiative decay rates regardless of the phase. Since phosphorescence was observed from DArNps, the k_{nr} values are attributed to intersystem crossing from the S_1 state to the triplet state. The triplet

TABLE 1 Photophysical parameters in chloroform, acetonitrile, and the solid state at 295 K for DArNps studied in the present work.^a

Compound	$\lambda_f^{~0-0}/nm$	$\Phi_{ m f}$	$ au_{ m f}/{ m ns}$	$k_{ m f}^{\ b}/10^7\ { m s}^{-1}$	$k_{ m nr}^{\ \ c}/10^7\ { m s}^{-1}$	$E_{\mathrm{T}}^{}}$ /kcal mol $^{-1}$
DPhNp	359 (359) ^e [380] ^e	0.17 (0.15) ^e [0.76] ^e	6.5 (32.0) ^e [12.0] ^e	2.6 (0.5) ^e [6.3] ^e	12.8 (2.7) ^e [2.0] ^e	54.7 ^e
PhPyNp	364 (364) [402]	0.45 (0.45) [0.20]	3.8 (5.5) [1.5]	11.8 (8.2) [13.3]	14.5 (10.0) [53.3]	54.7
DPyNp	364 (365) [393]	0.31 (0.39) [0.27]	4.3 (5.9) [1.6]	7.2 (6.6) [16.9]	16.0 (10.3) [45.6]	54.6

^aData in parentheses and brackets are for acetonitrile and the solid state.

eData from reference.7

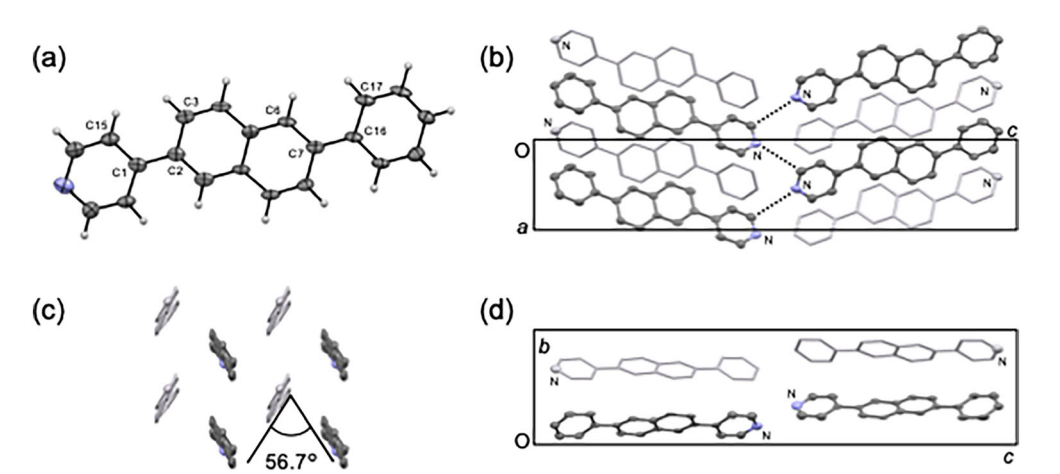


FIGURE 2 Crystal features of PhPyNp. 'N' indicates pyridine nitrogen. (a) ORTEP as drawing of the PhPyNp unit. (b) View along the *b*-axis. The dotted lines indicate nearest C–H...N contacts between chromophores. (c) View along the [01] direction. (d) View along the *a*-axis.

2192649, 0, Downloaded from https://onlinelibrary.wiley.com/doi/10.1002/jccs.70063 by Okayama University, Wiley Online Library on [2608/2025]. See the Terms and Conditions (https://onlinelibrary.wiley.com/terms-and-conditions) on Wiley Online Library for rules of use; OA articles are governed by the applicable Creative Commons Licenseon (https://onlinelibrary.wiley.com/terms-and-conditions) on Wiley Online Library for rules of use; OA articles are governed by the applicable Creative Commons Licenseon (https://onlinelibrary.wiley.com/terms-and-conditions) on Wiley Online Library for rules of use; OA articles are governed by the applicable Creative Commons Licenseon (https://onlinelibrary.wiley.com/terms-and-conditions) on Wiley Online Library for rules of use; OA articles are governed by the applicable Creative Commons Licenseon (https://onlinelibrary.wiley.com/terms-and-conditions) on Wiley Online Library for rules of use; OA articles are governed by the applicable Creative Commons Licenseon (https://onlinelibrary.wiley.com/terms-and-conditions) on Wiley Online Library for rules of use; OA articles are governed by the applicable Creative Commons Licenseon (https://onlinelibrary.wiley.com/terms-and-conditions) on Wiley Online Library for rules of use; OA articles are governed by the applicable Creative Commons Licenseon (https://onlinelibrary.wiley.com/terms-and-conditions) on Wiley Online Library for rules of use; OA articles are governed by the applicable Creative Commons Licenseon (https://onlinelibrary.wiley.com/terms-and-conditions) on Wiley Online Library for rules of use; OA articles are governed by the applicable Creative Commons Licenseon (https://onlinelibrary.wiley.com/terms-and-conditions) on Wiley Online Library for rules of use; OA articles are governed by the applicable Creative Commons Licenseon (https://onlinelibrary.wiley.com/terms-and-conditions) on Wiley Online Library for rules of use; OA articles are governed by the applicable Creative Commons Licenseon (https://onlinelibrary.wiley.com/term

energies, $E_{\rm T}$, determined from the phosphorescence origins are comparable and summarized in Table 1.

Previously, we reported that the fluorescence spectrum of DPhNp in the solid state is red-shifted relative to that in cyclohexane solution, and that its crystal packing adopts a herringbone motif [7]. It is of interest to analyze the crystal structures of PhPyNp and DPyNp for examining our hypothesis of correlation between emission spectra and crystal structures.

3.2 | X-ray crystallographic analysis of crystals

The crystal structures of PhPyNp and DPyNp were analyzed by X-ray diffraction in this work, whereas that of DPhNp was reported in our previous paper [7]. PhPyNp was obtained as a platelet crystal. Figure 2 shows the crystal structure of PhPyNp (CCDC 2452168). The molecules were arranged in a herringbone manner within the *ac* plane (Figure 2b). The top layer (dark gray) and the adjacent lower layer (light gray) are slip-stacked at a distance of 3.72 Å. As

shown in Figure 2c, inter-layer molecules are tilted at 56.7° . Therefore, the π - π interaction between the naphthalene moieties is negligible. The distance between pyridine nitrogen and the nearest C–H carbon atom indicated by the dotted line in Figure 2b is $3.52\,\text{Å}$, which is longer than the sum of van der Waals radii $(3.25\,\text{Å})$, showing no C–H...N hydrogen bonding interaction. Torsion angles between the phenyl and naphthalene rings were 11.8° and 13.5° .

DPyNp was also obtained as a platelet crystal. Figure 3 shows the crystal structure of DPyNp (CCDC 2452169). As shown in Figure 3b, the molecules are arranged in a herringbone manner as PhPyNp within the bc plane. The top layer (dark gray) and the adjacent lower layer (light gray) were slip-stacked with a distance of 3.46 Å, and no specific interaction such as π - π stacking was found between the naphthalene moieties. In addition, the distance between a pyridine nitrogen atom and the nearest C–H carbon atom indicated by the dotted line in Figure 3b is 3.64 Å, which is longer than the sum of van der Waals radii (3.25 Å), showing no C–H...N hydrogen bonding interaction. Torsion angles between the pyridyl and naphthalene rings were 28.7° .

^bEvaluated by Equation (1).

^cEvaluated by Equation (2).

^dDetermines the phosphorescence origin.

21926549, 0, Downloaded from https://onlinelibrary.wiley.com/doi/10.1002/jccs.70063 by Okayama University, Wiley Online Library on [26/08/2025]. See the Terms and Conditions

ons) on Wiley Online Library for rules of use; OA articles are governed by the applicable Creative Commons License

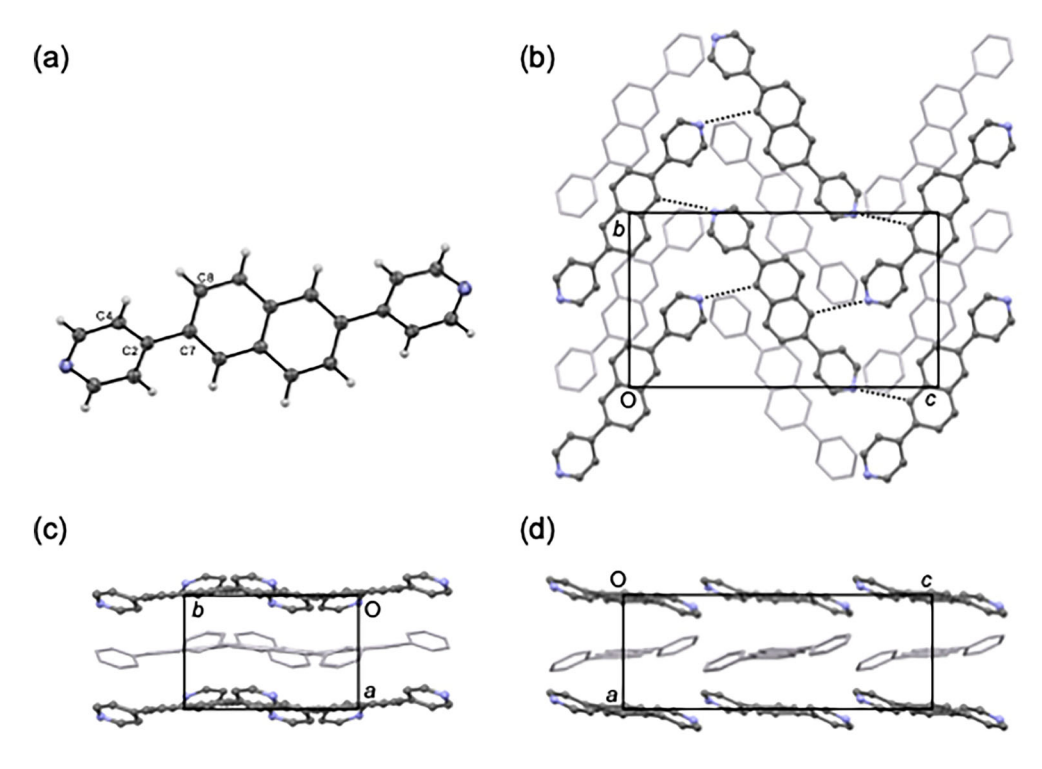


FIGURE 3 Crystal features of DPyNp. (a) ORTEP drawing of the DPyNp unit. (b) View along the a-axis showing the top layer (dark gray) and the lower layer (light gray) of the bc planes. The dotted lines indicate nearest C–H...N contacts between chromophores. (c) View along the b-axis. (d) View along the c-axis.

TABLE 2 Calculated photophysical parameters in chloroform for the studied DArNps. a

1								
Compound	HOMO/eV	LUMO/eV	$\lambda_{ m tr}^{ m f b}/{ m nm}$	f^c	$Coefficient \ of \ the \ S_1 \leftarrow S_0 \ transition^d$			
DPhNp	-5.93 [-5.73]	-1.71 [-1.63]	327 [331]	0.5925 [0.5229]	$\begin{array}{l} 0.69543~(H\to L)\\ [-0.11884~(H\text{-}1\to L+1)\\ 0.68200~(H\to L)\\ -0.10898~(H\to L+1)] \end{array}$			
PhPyNp	-5.97 [-5.94]	-2.11 [-2.13]	359 [352]	0.8710 [0.8008]	0.70056 (H $ ightarrow$ L) [0.69669 (H $ ightarrow$ L)]			
DPyNp	-5.79 [-6.32]	-1.47 [-2.19]	319 [330]	0.3627 [0.4082]	$\begin{array}{l} 0.69714(H\to L)\\ [0.15164(H\text{-}1\to L)\\ -0.12039(H\text{-}1\to L+1)\\ 0.66808(H\to L)\\ 0.11197(H\to L+1)] \end{array}$			

^aIn brackets, calculated data based on the single crystal structures.

In brief, the crystal motifs of PhPyNp and DPyNp were found to be herringbone, as we expected from the solid-state emission shifts.

3.3 | Quantum chemical calculation

To gain deeper insight into the photophysical properties of the studied DArNps, DFT and TD-DFT calculations

were carried out at the (TD)-B3LYP/6–31 + G(d) level, considering chloroform as the solvent [28]. The calculation results are summarized in Table 2. The molecular orbital diagrams of the highest occupied molecular orbitals (HOMO) and lowest unoccupied molecular orbitals (LUMO) in chloroform are shown in Figure 4. In the optimized structures of DArNps, the HOMO and LUMO are located on the chromophoric regions. The transition wavelengths (λ_{tr}) estimated from

^bWavelength estimated from the transition energy.

 $^{^{}c}$ Oscillator strength of the $S_{1} \leftarrow S_{0}$ transition.

^dH and L denote the HOMO and LUMO, respectively.

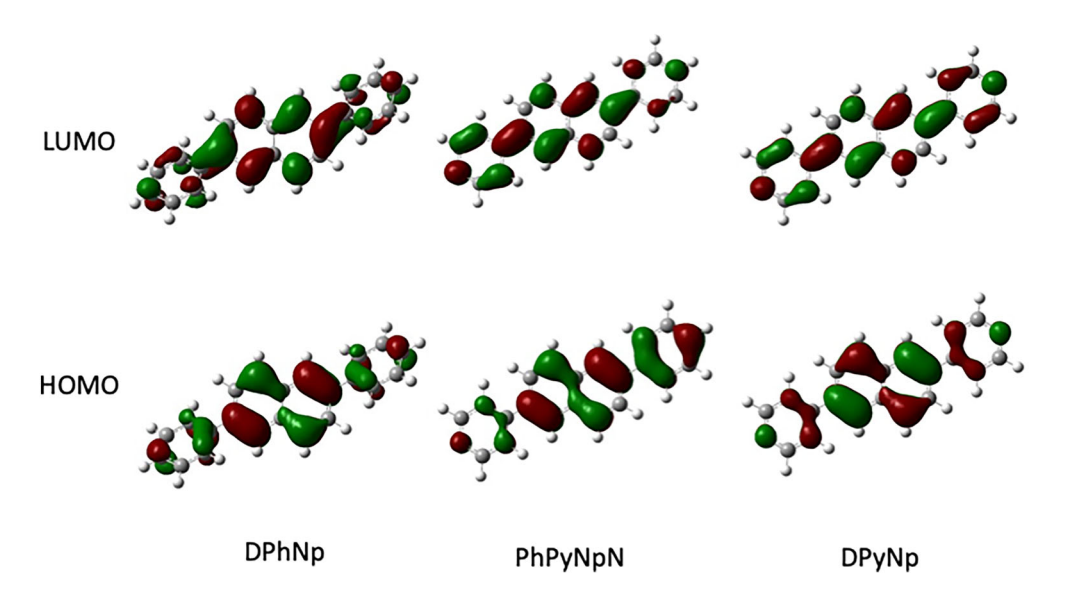


FIGURE 4 HOMO and LUMO surfaces of the studied DArNps in chloroform.

the excitation energies fall within the 320-360 nm range. The calculated oscillator strength (f) for the $S_1 \leftarrow S_0$ transitions confirms that these are allowed electronic transitions. On the other hand, based on their single crystal data, we also analyzed the HOMO and LUMO characteristics of DArNps in the single crystals for comparison with those obtained in chloroform. The corresponding computed values for the single crystal structures are listed in Table 2, and the visualized HOMO and LUMO surfaces are provided in Figure S7. The HOMO and LUMO distributions in the single crystals are similarly localized on the chromophores as seen in chloroform (Figure 4). The energy levels of HOMO and LUMO in the single crystals for DPhNp and PhPyNp closely resemble those in chloroform, whereas those of DPyNp are noticeably stabilized in the single crystal. This stabilization in the single crystal of DPyNp is reflected in the lower calculated wavelengths (λ_{tr}), which is consistent with the low-energy shift in the emission spectra observed in the present study.

4 | CONCLUSIONS

Building on our previous research, in which we observed solid-state emission from biaryls and diphenylnaphthalenes bearing multiple chromophores [6, 7], we hypothesized that such PAHs would exhibit solid-state fluorescence. In some cases, these compounds showed red-shifted emission spectra in the solid state compared with those in solution. Furthermore, the single-crystal structure of DPhNp was found to adopt a herringbone packing motif. These findings led us to focus on the correlation between crystal packing arrangements and

emission spectral characteristics in the present study. In this study, we investigated the photophysical properties and crystal structures of two naphthalene derivatives, PhPyNp and DPyNp, bearing phenyl and/or pyridyl substituents, with a focus on understanding the relationship between solid-state photoluminescence and molecular packing motifs. Both compounds exhibited red-shifted emission in the solid state compared with their emission in solution, consistent with the behavior observed for DPhNp. X-ray crystallographic analysis revealed that PhPyNp and DPyNp adopt herringbone-type packing motifs without significant intermolecular π - π stacking, supporting the hypothesis that herringbone packing is correlated with red-shifted solid-state emission.

Photophysical measurements showed that substitution with pyridyl groups increases the $k_{\rm f}$ values, while phosphorescence observations indicate efficient intersystem crossing to the triplet state. Quantum chemical calculations further confirmed that the electronic transitions are localized on the chromophores, and that the solid-state environment, particularly for DPyNp, leads to stabilization of the frontier molecular orbitals, in agreement with the observed spectral red shifts.

Taken together, these experimental results support a structure–property relationship in which the presence of a herringbone crystal packing motif is predictive of redshifted solid-state fluorescence in PAHs of multiple chromophores. This correlation provides a useful criterion for screening and designing new luminescent organic materials, particularly for optoelectronic applications such as organic semiconductors, where both emission efficiency and favorable molecular packing are critical. The semiconducting properties of DArNps should be explored in future work.

JCCS

ACKNOWLEDGMENTS

This research was funded by Grant-in-Aids for Scientific Research (JP18H02043, JP20K05648 and JP23K04877) from the Japan Society for the Promotion of Science (JSPS) to MY and HO, and General Incorporated Foundation Monodzukuri Research Organization (MRO), established by Ota Chamber of Commerce & Industry, Gunma University and Ota City in Gunma, Japan. MY acknowledges the technical staff at Kyushu University for performing the HRMS spectrometry of BrPyNp and PhPyNp under the Cooperative Research Program of the Network Joint Research Center for Materials and Devices.

DATA AVAILABILITY STATEMENT

The data that supports the findings of this study are available in the supplementary material of this article.

ORCID

Minoru Yamaji https://orcid.org/0000-0001-9963-2136

Fumito Tani https://orcid.org/0000-0002-9166-2127

Hideki Okamoto https://orcid.org/0000-0002-8742-4089

REFERENCES

- J. B. Birks, Photophysics of Aromatic Molecules, Wiely-Interscience, London 1970.
- [2] J. R. Lakowicz, J. R. Lakowicz, J. R. Lakowicz, Principle of Fluorescence Spectroscopy, 3rd ed., Springer, US 2006.
- [3] B. Valeur, B. Valeur, Molecular Fluorescence: Principles and Applications, 2nd ed., Wiely-VCH, Weinheim 2013.
- [4] R. Katoh, K. Suzuki, A. Furube, M. Kotani, K. Tokumaru, R. Katoh, K. Suzuki, A. Furube, M. Kotani, K. Tokumaru, R. Katoh, K. Suzuki, A. Furube, M. Kotani, K. Tokumaru, *J. Phys. Chem. C* **2009**, *113*, 2961.
- [5] K. Suzuki, A. Kobayashi, S. Kaneko, K. Takehira, T. Yoshihara, H. Ishida, Y. Shiina, S. Oishi, S. Tobita, K. Suzuki, A. Kobayashi, S. Kaneko, K. Takehira, T. Yoshihara, H. Ishida, Y. Shiina, S. Oishi, S. Tobita, K. Suzuki, A. Kobayashi, S. Kaneko, K. Takehira, T. Yoshihara, H. Ishida, Y. Shiina, S. Oishi, S. Tobita, *Phys. Chem. Chem. Phys.* 2009, 11, 9850.
- [6] M. Yamaji, H. Okamoto, K. Goto, F. Tani, M. Yamaji, H. Okamoto, K. Goto, F. Tani, M. Yamaji, H. Okamoto, K. Goto, F. Tani, J. Photochem. Photobiol. A 2021, 421, 113518.
- [7] M. Yamaji, T. Mutai, I. Yoshikawa, H. Houjou, H. Okamoto, M. Yamaji, T. Mutai, I. Yoshikawa, H. Houjou, H. Okamoto, M. Yamaji, T. Mutai, I. Yoshikawa, H. Houjou, H. Okamoto, Molecules 2024, 29, 5941.
- [8] X. Q. Sun, G. Y. Qin, P. P. Lin, J. Wang, J. X. Fan, H. Y. Li, A. M. Ren, J. F. Guo, X. Q. Sun, G. Y. Qin, P. P. Lin, J. Wang, J. X. Fan, H. Y. Li, A. M. Ren, J. F. Guo, X. Q. Sun, G. Y. Qin, P. P. Lin, J. Wang, J. X. Fan, H. Y. Li, A. M. Ren, J. F. Guo, *Phys. Chem. Chem. Phys.* 2021, 23, 12679.
- [9] M. Liu, Y. Wei, Q. Ou, P. Yu, G. Wang, Y. Duan, H. Geng, Q. Peng, Z. Shuai, Y. Liao, M. Liu, Y. Wei, Q. Ou, P. Yu, G. Wang, Y. Duan, H. Geng, Q. Peng, Z. Shuai, Y. Liao, M. Liu, Y. Wei, Q. Ou, P. Yu, G. Wang, Y. Duan, H. Geng, Q. Peng, Z. Shuai, Y. Liao, J. Phys. Chem. Lett. 2021, 12, 938.

- [10] Z. Qin, H. Gao, J. Liu, K. Zhou, J. Li, Y. Dang, L. Huang, H. Deng, X. Zhang, H. Dong, W. Hu, Z. Qin, H. Gao, J. Liu, K. Zhou, J. Li, Y. Dang, L. Huang, H. Deng, X. Zhang, H. Dong, W. Hu, Z. Qin, H. Gao, J. Liu, K. Zhou, J. Li, Y. Dang, L. Huang, H. Deng, X. Zhang, H. Dong, W. Hu, Adv. Mater. 2019, 31, e1903175.
- [11] J. Liu, J. Liu, Z. Zhang, C. Xu, Q. Li, K. Zhou, H. Dong, X. Zhang, W. Hu, J. Liu, J. Liu, Z. Zhang, C. Xu, Q. Li, K. Zhou, H. Dong, X. Zhang, W. Hu, J. Liu, J. Liu, Z. Zhang, C. Xu, Q. Li, K. Zhou, H. Dong, X. Zhang, W. Hu, J. Mater. Chem. C 2017, 5, 2519.
- [12] J. Fan, L. Lin, C. K. Wang, J. Fan, L. Lin, C. K. Wang, J. Fan, L. Lin, C. K. Wang, Phys. Chem. Chem. Phys. 2017, 19, 30147.
- [13] J. Liu, H. Zhang, H. Dong, L. Meng, L. Jiang, L. Jiang, Y. Wang, J. Yu, Y. Sun, W. Hu, A. J. Heeger, J. Liu, H. Zhang, H. Dong, L. Meng, L. Jiang, L. Jiang, Y. Wang, J. Yu, Y. Sun, W. Hu, A. J. Heeger, J. Liu, H. Zhang, H. Dong, L. Meng, L. Jiang, L. Jiang, Y. Wang, J. Yu, Y. Sun, W. Hu, A. J. Heeger, *Nat. Commun.* 2015, 6, 10032.
- [14] G. Qin, P. Lin, X. Sun, J. Guo, J. Fan, L. Ji, H. Li, A. Ren, G. Qin, P. Lin, X. Sun, J. Guo, J. Fan, L. Ji, H. Li, A. Ren, G. Qin, P. Lin, X. Sun, J. Guo, J. Fan, L. Ji, H. Li, A. Ren, *Phys. Chem. Chem. Phys.* 2023, 25, 540.
- [15] G. Bolla, J. Guo, H. Zhao, S. Lv, J. Liu, Y. Li, Y. Zhen, Q. Liao, X. Wang, H. Fu, H. Dong, Z. Wang, Z. Wang, W. Hu, G. Bolla, J. Guo, H. Zhao, S. Lv, J. Liu, Y. Li, Y. Zhen, Q. Liao, X. Wang, H. Fu, H. Dong, Z. Wang, Z. Wang, W. Hu, G. Bolla, J. Guo, H. Zhao, S. Lv, J. Liu, Y. Li, Y. Zhen, Q. Liao, X. Wang, H. Fu, H. Dong, Z. Wang, Z. Wang, W. Hu, CrystEngComm 2022, 24, 5683
- [16] X. Ran, M. Akbar Ali, X.-Z. Peng, G.-J. Yu, J.-Y. Ge, L. Yang, Y. Chen, L.-H. Xie, X. Ran, M. Akbar Ali, X.-Z. Peng, G.-J. Yu, J.-Y. Ge, L. Yang, Y. Chen, L.-H. Xie, X. Ran, M. Akbar Ali, X.-Z. Peng, G.-J. Yu, J.-Y. Ge, L. Yang, Y. Chen, L.-H. Xie, New J. Chem. 2022, 46, 1135.
- [17] J. Liu, W. Zhu, K. Zhou, Z. Wang, Y. Zou, Q. Meng, J. Li, Y. Zhen, W. Hu, J. Liu, W. Zhu, K. Zhou, Z. Wang, Y. Zou, Q. Meng, J. Li, Y. Zhen, W. Hu, J. Liu, W. Zhu, K. Zhou, Z. Wang, Y. Zou, Q. Meng, J. Li, Y. Zhen, W. Hu, J. Mater. Chem. C 2016, 4, 3621.
- [18] L. Zhao, J. Li, L. Li, W. Hu, L. Zhao, J. Li, L. Li, W. Hu, L. Zhao, J. Li, L. Li, W. Hu, J. Mater. Chem. C 2024, 12, 13745.
- [19] C. Wang, H. Dong, W. Hu, Y. Liu, D. Zhu, C. Wang, H. Dong, W. Hu, Y. Liu, D. Zhu, C. Wang, H. Dong, W. Hu, Y. Liu, D. Zhu, Chem. Rev. 2012, 112, 2208.
- [20] J. E. Anthony, J. E. Anthony, J. E. Anthony, Chem. Rev. 2006, 106, 5028.
- [21] C. Wang, H. Dong, L. Jiang, W. Hu, C. Wang, H. Dong, L. Jiang, W. Hu, C. Wang, H. Dong, L. Jiang, W. Hu, Chem. Soc. Rev. 2018, 47, 422.
- [22] S. Fujino, M. Yamaji, H. Okamoto, T. Mutai, I. Yoshikawa, H. Houjou, F. Tani, S. Fujino, M. Yamaji, H. Okamoto, T. Mutai, I. Yoshikawa, H. Houjou, F. Tani, S. Fujino, M. Yamaji, H. Okamoto, T. Mutai, I. Yoshikawa, H. Houjou, F. Tani, *Photochem. Photobiol. Sci.* 2017, 16, 925.
- [23] M. Yamaji, S. Kato, K. Tomonari, M. Mamiya, K. Goto, H. Okamoto, Y. Nakamura, F. Tani, M. Yamaji, S. Kato, K. Tomonari, M. Mamiya, K. Goto, H. Okamoto, Y. Nakamura, F.

- Tani, M. Yamaji, S. Kato, K. Tomonari, M. Mamiya, K. Goto, H. Okamoto, Y. Nakamura, F. Tani, *Inorg. Chem.* **2017**, *56*, 12514.
- [24] M. Yamaji, K. Tomonari, K. Ikuma, K. Goto, F. Tani, H. Okamoto, M. Yamaji, K. Tomonari, K. Ikuma, K. Goto, F. Tani, H. Okamoto, M. Yamaji, K. Tomonari, K. Ikuma, K. Goto, F. Tani, H. Okamoto, *Photochem. Photobiol. Sci.* 2019, 18, 2884.
- [25] G. M. Sheldrick, G. M. Sheldrick, G. M. Sheldrick, Acta Cryst. A 2008, 72, 112.
- [26] G. Sheldrick, G. Sheldrick, Acta Crystallogr. C 2015, 71, 3.
- [27] C. Kabuto, S. Akine, T. Nemoto, E. Kwon, C. Kabuto, S. Akine, T. Nemoto, E. Kwon, C. Kabuto, S. Akine, T. Nemoto, E. Kwon, J. Cryst. Soc. Jpn. 2009, 51, 218.
- [28] M. J. Frisch, G. W. Trucks, H. B. Schlegel, G. E. Scuseria, M. A. Robb, J. R. Cheeseman, G. Scalmani, V. Barone, B. Mennucci, G. A. Petersson, H. Nakatsuji, M. Caricato, X. Li, H. P. Hratchian, A. F. Izmaylov, J. Bloino, G. Zheng, J. L. Sonnenberg, M. Hada, M. Ehara, K. Toyota, R. Fukuda, J. Hasegawa, M. Ishida, T. Nakajima, Y. Honda, O. Kitao, H. Nakai, T. Vreven, J. J. A. Montgomery, J. E. Peralta, F. Ogliaro, M. Bearpark, J. J. Heyd, E. Brothers, K. N. Kudin, V. N. Staroverov, T. Keith, R. Kobayashi, J. Normand, K.

Raghavachari, A. Rendell, J. C. Burant, S. S. Iyengar, J. Tomasi, M. Cossi, N. Rega, J. M. Millam, M. Klene, J. E. Knox, J. B. Cross, V. Bakken, C. Adamo, J. Jaramillo, R. Gomperts, R. E. Stratmann, O. Yazyev, A. J. Austin, R. Cammi, C. Pomelli, J. W. Ochterski, R. L. Martin, K. Morokuma, V. G. Zakrzewski, G. A. Voth, P. Salvador, J. J. Dannenberg, S. Dapprich, A. D. Daniels, O. Farkas, J. B. Foresman, J. V. Ortiz, J. Cioslowski, D. J. Fox, *Gaussian 09, Revision D.01*, Gaussian, Inc, Wallingford CT **2010**.

SUPPORTING INFORMATION

Additional supporting information can be found online in the Supporting Information section at the end of this article.

How to cite this article: M. Yamaji, I. Yoshikawa, T. Mutai, H. Houjou, K. Goto, F. Tani, K. Suzuki, H. Okamoto, *J. Chin. Chem. Soc.* **2025**, 1. https://doi.org/10.1002/jccs.70063